Design of a Synchronous Reluctance Motor with Non-Overlapping Fractional-Slot Concentrated Windings

Christopher Spargo
Member, IEEE
School of Electrical and Electronic Engineering,
Newcastle University, United Kingdom
c.m.spargo@ncl.ac.uk

Barrie Mecrow
Member, IEEE
School of Electrical and Electronic Engineering,
Newcastle University, United Kingdom
barrie.mecrow@ncl.ac.uk

James Widmer
School of Electrical and Electronic Engineering,
Newcastle University, United Kingdom
james.widmer@ncl.ac.uk

***Abstract* -- This paper presents the detailed design and finite element study of a synchronous reluctance machine with a non-overlapping fractional slot concentrated windings. The machine design employs single tooth wound coils with short end windings and high fill factor, which facilitates the machines high torque density and efficiency. As no magnets are required, the machine is low cost and of robust construction like the induction motor. This machine topology is presented as a step forward in synchronous reluctance technology which are usually wound with a distributed winding with long end turns. Analytical design methodologies and performance through finite element studies are presented. Scaling and design options, along with manufacturing options are discussed, the future development of the topology for automotive traction and other demanding applications is also presented.**

***Index Terms*-- AC motor, concentrated winding, non-overlapping winding, synchronous reluctance machine.**

I. Introduction

Ever since the introduction of the transversely laminated topology synchronous reluctance motor in 1924, they have been wound with polyphase distributed windings [1-4]. These windings are often laborious to wind and have very long mean end turn lengths, the consequence is redundant copper mass and corresponding stator winding Joule loss. These windings also typically have a low slot fill, leading to low torque density and low efficiency when compared to machine with higher fills. The use of fractional slot concentrated windings (FSCW) in synchronous reluctance machines is a logical step to realizing a higher torque density and efficiency machine [5, 11]. Application of FSCW reduces the mean end turn length, reducing both machine mass and copper loss, a benefit of which the switched reluctance motor has due to its tooth concentrated coils [6]. As such, there are many advantages to designing a synchronous reluctance machine with fractional slot concentrated windings [5] which tend increase as the rotor pole number increases [7]. Increased power density and energy conversion efficiency can be achieved over that of a conventional SynRM, with improved thermal properties, easier and lower cost manufacturing, which are very robust, such as the induction motor. This is facilitated by the short end windings and attainable high slot fill factors assisted by segmentation of the stator component [8]. However, very low power factors and high torque ripple were alluded due to a high level of MMF space harmonic content. The presented topology is similar to that of a switched reluctance motor (SRM), but is a true AC machine fed by a conventional voltage source inverter, unlike the switched reluctance machine which requires a non-standard converter, has more complicated control schemes and generally high torque ripple [6]. Figure 1 shows a half FE model of a cSynRM, a fractional slot concentrated winding synchronous reluctance machine with 6 slot and 4 poles.

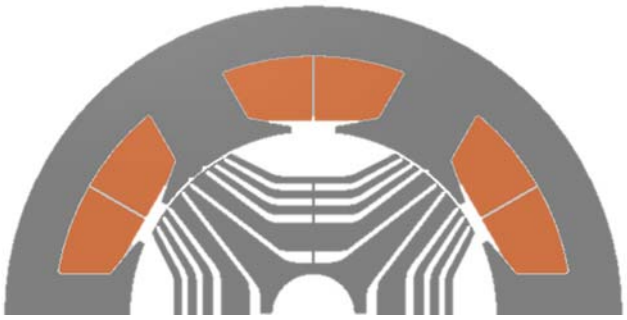

Fig. 1. A 6-slot 4-pole synchronous reluctance machine with fractional slot concentrated windings.

This paper details the analytical design and finite element validation of a high torque density, high efficiency synchronous reluctance machine equipped with fractional slot concentrated windings.

II. Specification

The machine is designed with a casing bore of 150mm and axial length of 200mm. The machine has cooling fins but no forced ventilation so is of the totally enclosed no ventilation

type. The outer active material dimensions are chosen to be comparable to other machines in-house machines designed for research purposes. The stator stack length is 150mm with an outside stator diameter of 150mm. The machines base speed is chosen to be 1500 rpm at a DC link voltage of 560V, a three phase machine is considered with fractional slot concentrated windings.

III. Stator and Winding Design

In this section, analytical design work is carried to find the approximate machine dimensions, which are finalized through finite element studies.

A. Stator Winding Specification

Now that the extreme machine dimensions are selected, the details of the stator design must be chosen. The machine is three-phase ($m = 3$) and is designed with a fractional slot concentrated winding which utilizes a single tooth span and are therefore not overlapping in the end region. The applicable slot-pole combinations that support fractional slot concentrated windings are limited for P<6, as represented in Table II.

TABLE II
APPLICABLE SLOT-POLE COMBINATIONS (WINDING FACTORS)

	Number of Poles		
Number of Slots	***2***	***4***	***6***
3	0.866	0.866	
6		**0.866**	
9		0.617	0.866

It is aimed to maximize the winding factor k_{w1} and minimize the space harmonic content. A double layer winding is selected $n_l = 2$. For a four pole machine, $p = 2$ with a slot number $Q_s = 6$ which supports a fractional slot concentrated winding, the number of slots per pole;

$$q = \frac{Q_s}{2mp} = \frac{1}{2} < 1 \tag{1}$$

Due to the even denominator of Eq. (1), the winding is classified as a Grade I winding with applicable harmonic ordinates [5];

$$v = \frac{1}{n}(6g + 2); \text{where } g = 1,2,3,4 \ldots \tag{2}$$

The harmonics take on the values, 1, -2, 4, -5, 7 … etc. The – ve indicates that these harmonics are counter-rotating harmonics with respect to the fundamental field. Odd and even harmonic ordinals exist due to air gap flux asymmetry over a rotor pole pitch. The winding factors can then be analytically determined;

$$k_{wv} = \sin\left(\frac{\pi p}{Q_s}\right)\frac{\sin\left(\frac{v\pi}{2m}\right)}{nq\sin\left(\frac{v\pi}{2mnq}\right)} \tag{3}$$

Thus by substitution $k_w = 0.866 = \text{constant}$. The harmonic winding factors are equal to that of the fundamental torque producing factor, leading to high space harmonic content. The winding factors and the resultant three phase MMF harmonics are presented in Figure. 2. The winding layout is presented in Figure. 3 and the airgap periphery MMF distribution of a single phase is presented in Figure. 4.

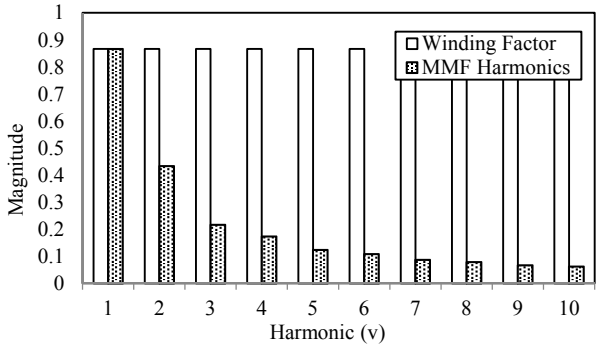

Fig.2. Winding factors and MMF harmonics of a cSynRM with a double layer fractional slot concentrated winding of 6 slots and 4 poles.

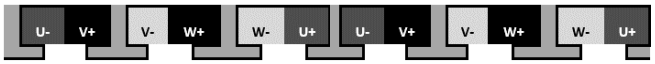

Fig.3. Winding layout of the 6-slot 4-pole double layer fractional slot concentrated winding, (repeated twice for full winding)

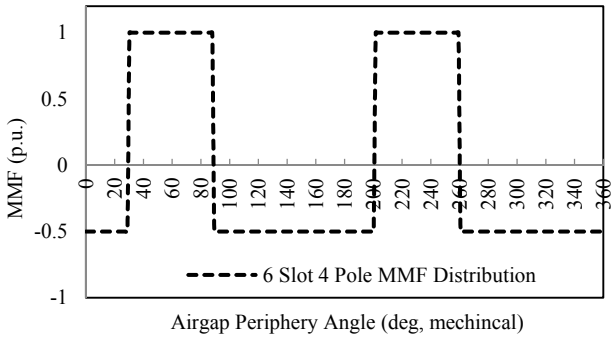

Fig. 4. MMF distribution function of the 6-slot 4-pole fractional slot concentrated winding synchronous reluctance machine (Three Phases).

B. Optimum Rotor Outer Diameter

With the stator outer diameter D_{so} set at 150mm, the optimum rotor outer diameter D_{ro} must firstly be calculated to give optimum performance. The torque output of a machine is proportional to the product of the rotor volume V_r and electric loading A. There is a tradeoff between the rotor volume and electric loading in relation to the slot inner D_{ssi} and outer D_{sso} diameters for maximum torque production. A larger D_{ro} increases the rotor volume but reduces the slot area available for the stator windings for a given D_{sso}. Using the ratio;

$$\beta = \frac{D_{ssi}}{D_{sso}} \tag{4}$$

the per-unit torque production can be written (for parallel teeth);

$$T = \beta^2(1 - \beta^2) \tag{5}$$

As the electric loading is approximately proportional to the area between the stator slot inner and outer diameters. From differential calculus, $\frac{dT}{d\beta} = \frac{d}{d\beta}\left[\beta^2(1-\beta^2)\right] = 0$, for a local maximum such that a cubic equation is required to be solved for optimum β, it is readily calculated that the optimum ratio is;

$$\beta = \frac{D_{ssi}}{D_{sso}} = \frac{\sqrt{2}}{2} \tag{6}$$

Equation 6 is depicted graphically in Figure 5.

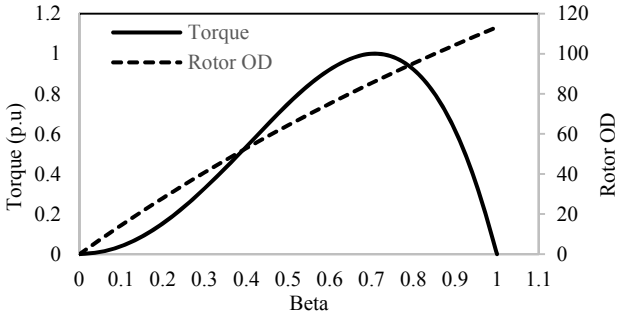

Fig. 5. Machine torque as a function of the ratio β.

Through development of the machine sizing equations, it can be shown that the optimum rotor outer diameter can be approximated;

$$D_{ro} \cong \frac{\beta D_{so} - 2\delta}{1 + \beta k_1\left(\frac{\pi}{2p}\right)} \qquad \mathrm{k_1} \triangleq \frac{\widehat{\mathrm{B}}_{\delta 1}}{\widehat{\mathrm{B}}_{\mathrm{cb}}} \tag{7}$$

Where δ is the airgap length, k_1 is a constant determined by magnetic loading and p the number of pole pairs. The rotor optimal diameter is approximated as 85mm.

C. Stator Dimensions

With the optimum rotor outer diameter calculated D_{ssi}, D_{sso} and the coreback depth t_{cb} are readily found by the following relations;

$$D_{ssi} = D_{ro} + 2\delta \quad ; \quad D_{sso} = \frac{D_{ssi}}{\beta} \tag{8}$$

$$t_{cb} = \frac{D_{so} - D_{sso}}{2} \tag{9}$$

Which are calculated as 86mm, 122mm and 14mm. The tooth width is calculated from the relation;

$$\mathrm{t_t} = \frac{\mathrm{k_s}\pi \mathrm{D_\delta}}{\mathrm{Q_s}} \qquad \mathrm{k_2} \triangleq \frac{\widehat{\mathrm{B}}_{\delta 1}}{\widehat{\mathrm{B}}_{\mathrm{t}}} \tag{10}$$

The constant $\mathrm{k_2} = 0.437$ such that the tooth width is then approximately 21mm. Where, $\widehat{\mathrm{B}}_{\delta 1}$ is the peak fundamental airgap flux density, $\widehat{\mathrm{B}}_{\mathrm{cb}}$ and $\widehat{\mathrm{B}}_{\mathrm{t}}$ are the permissible flux densities in the stator coreback and middle of the stator teeth respectively.

D. Stator Winding Parameters

A six slot, four pole factional slot concentrated winding was specified in *Subsection A*. The stator slot and rotor pole pitches are calculated (assuming $D_{ssi} = D_{ro} = D_\delta$ of 86mm);

$$\tau_u = \frac{\pi D_\delta}{6qp} \quad ; \quad \tau_p = \frac{\pi D_\delta}{2p} \tag{11}$$

Which equate to 46.6mm and 69.9mm respectively. With the dimensions set, details of windings must be determined. A double layer winding is used as this minimizes the harmonic content. The chosen DC link voltage $\mathrm{V_{DC}} = 590\mathrm{V}$ corresponding to the specification., with a rated speed of 1500 $\mathrm{min^{-1}}$, the maximum phase voltage $\mathrm{V_{Ph}}$, assuming a DC link utilization of 95%, with a star connected winding is given as;

$$\frac{0.95\mathrm{V_{DC}}}{\sqrt{3}} = \widehat{\mathrm{V_{Ph}}} \tag{12}$$

Accordingly, the number of series turns per phase for an operating peak flux per pole $\hat{\phi}$ at base speed $\mathrm{n_{base}}$ is determined;

$$\mathrm{N_s} = \mathrm{integer}\left|\frac{60\widehat{\mathrm{V_{Ph}}}}{2\pi p k_w \mathrm{k_i}\widehat{\mathrm{B}}_{\delta 1}\tau_\mathrm{p}\mathrm{l}'\,\mathrm{n_{base}}}\right| \tag{13}$$

Where $\mathrm{k_i}$ the waveform factor and $\mathrm{l}' = \mathrm{l} + 2\delta$ is the equivalent core length. The number of turns is approximated as 104 per phase. The turns per coil are then 52 turns. The winding layout presented in Figure. 3.

E. Performance

Taking a reasonable tangential stress $\sigma_{\tan}$ of a salient synchronous machine of 27kPa for a totally enclosed radial flux machine with unity power factor $\cos(\varphi) = 1$, this is modified as;

$$\sigma'_{\tan} = \sigma_{\tan}\cos(\varphi) \tag{14}$$

In a synchronous reluctance machine, the power factor for a given rotor saliency ratio ξ can be estimated under maximum torque per Ampere control;

$$\cos(\varphi) \approx \frac{\xi - 1}{\sqrt{2}}\sqrt{\frac{1}{\xi^2 + 1}} \tag{15}$$

For this size machine and due to the extra harmonic fluxes caused by the space harmonic content, a conservative estimate of the saliency ratio would be 4, giving a power factor of 0.45. This rates the actual tangential shear stress at around 13kPa from which the machine electromagnetic torque is derived;

$$\mathrm{T_{em}} = \left(\frac{\pi}{2}\right)\sigma'_{\tan}\mathrm{D_{ro}^2 l}' = 2\sigma'_{\tan}\mathrm{V_r} \tag{16}$$

Where V_r , is the rotor electromagnetic volume, so the estimate torque output for the machine is approximated at 23.1Nm at 1500rpm giving a rated power of just below 3.6kW. The rated current of the machine is determined by the electric and magnetic loadings in the machine;

$$A\widehat{B}_{\delta 1} = \frac{\sqrt{2}\sigma'_{\tan}}{\cos(\varphi)} \quad ; \quad I_s = \frac{\pi A D_\delta}{2mN_s} \tag{17}$$

Where $\widehat{B}_{\delta 1} = 0.8$, which is typical, the RMS linear electric loading is determined to be 47 kA/m. The rated RMS phase current is calculated as 21.2A. The mean turn length l_m determines the phase resistance R_{ph}. The phase resistance consists of two components, the axial portion and the end section;

$$R_{ph} = \frac{N_s \rho l_m}{A_{\text{slot}} k_{\text{fill}}} = \frac{2N_s \rho}{A_{\text{slot}} k_{\text{fill}}} (l + l_{\text{end}}) \tag{18}$$

Where A_{slot} is the slot area, k_{fill} is the slot fill factor, ρ is the winding material (copper) resistivity, l is the stack length and l_{end} is the mean end winding length. The length l_{end} for double layer concentrated windings can be approximated by [13];

$$l_{\text{end}} = 0.93\left(\frac{\pi r_w}{Q_s}\right) \tag{19}$$

Where $r_w \cong \frac{D_{sso} - D_{ssi}}{4} + \frac{D_{ssi}}{2}$ relates to the average coil radius, and the coil axial extent approximated by $l_{\text{axial}} = \frac{l_{\text{end}}}{\pi}$ for a semi-circular end winding. Finally the phase resistance can be determined as 220mOhm with an axial extent of 20mm assuming a fill factor of 60%, which is achievable. The approximate slot area is 560 mm^2. Calculations result in a 308W copper loss at rated current and if the iron loss can be assumed approximately 10% of the copper loss as the machine is low speed, the total loss is around 350W, resulting in an efficiency of 91%. This is very good for the power rating and size of the designed machine. Finite element studies are used to optimize the design based on the analytical solutions. The optimal tooth tip depth and stator tooth face span are determined to be 1.6mm and 46 degrees, as in Fig. 6

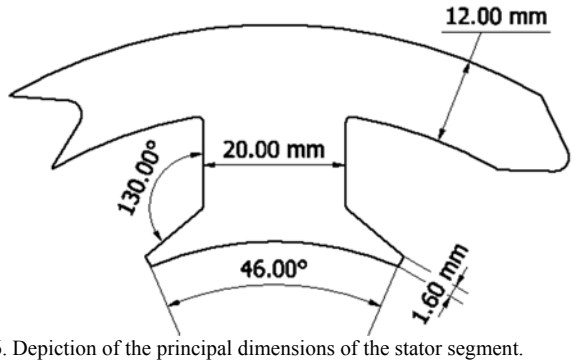

Fig.6. Depiction of the principal dimensions of the stator segment.

The stator is segmented to aid coil winding and ease of construction. The tooth can be wound before assembly resulting is high fill factors. In this machine, a slot fill factor of 60% is achieved. A shrink fit of the assembled stator into the case ensures that any small air gaps between segments are closed up as to not significantly affect machine performance.

IV. Rotor Design

The rotor design is very important in this machine as the high space harmonic content causes a large torque ripple [5]. Conventional design rules were obeyed, such as small radial and tangential ribs, an optimized number of barriers and insulation ratio of approximately 0.5. The rotor design is presented briefly here (with parameters in Table III) but is considered in detail and mathematically in [9].

TABLE III
Rotor Parameters

Parameter	Value
Rotor outer diameter [mm]	89
Active stack length [mm]	150
Number of barriers	4 + cutout
Number of layers	9
Insulation ratio (q-axis)	0.5
Saliency Ratio (Unsaturated)	4
Unsaturated d-axis inductance (mH)	28
Unsaturated q-axis inductance (mH)	6

The resultant tangential stress on the rotor surface can be written;

$$\sigma(\theta, t) = \frac{B_\theta(\theta, t) B_r(\theta, t)}{\mu_0} \tag{20}$$

Then from Maxwell Stress Tensor theory the resultant rotor electromagnetic torque at a time instant is given by integrating over the surface;

$$T_\theta(t) = \frac{r^2}{\mu_0} \int_0^{l_a} \int_0^{2\pi} \sigma(\theta, t)\, d\theta dz \tag{21}$$

Tangential and radial, $B_\theta(\theta, t)$ and $B_r(\theta, t)$, airgap fields contain harmonics, derived from the high MMF space harmonic content, this causes a large torque ripple as a manifested. In this machine slot pole combination, it is found [9] that the second order field harmonic, *which is 8-pole counter-rotating*, is the offending field. Thus reduction of the

interaction of this harmonic with the rotor is of importance.

Fig.7. Optimized rotor component.

As described in [9] simple rotor cutouts can reduce this saliency and improve the torque quality in the machine. The optimized rotor is presented in Figure 7.

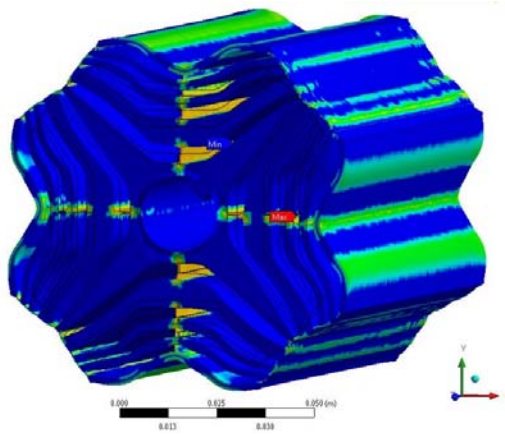

Fig.8. Mechanical finite element analysis – safety factor with exaggerated deformation (x1000).

Mechanical FE analysis predicts that the rotor is safe to 10,000 rpm (Fig. 8), minimum safety factor is 2. The radial and tangential rib thicknesses are 0.5mm and 0.3mm respectively, these thicknesses minimize the q-axis flux for high performance but will limit the maximum rotor speed.

V. Finite Element Analysis

Finite element analysis is used to verify the machines performance based on the analytical design. At the rated speed of the machine (1500rpm) the developed torque as a function of current angle and percentage line current from 10% to 130% is presented in Fig. 8. The rated current point is presented as a single point.

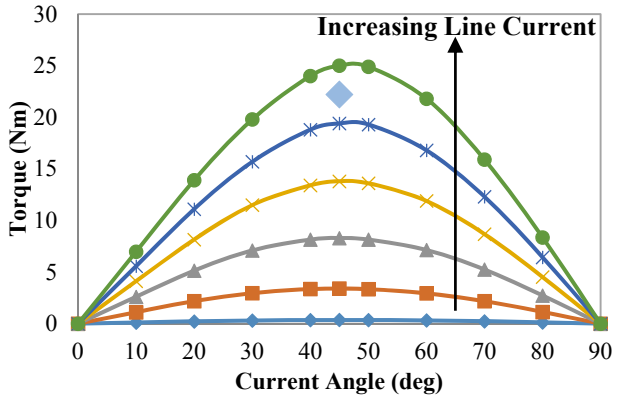

Fig.8. Torque vs. current angle for various line currents.

The machine produces an average of 23Nm at a rated current of 21A, compared to the calculated design value of 24.5Nm at 23A. The machine exhibits high torque density, greater than an identical size induction machine, conventional synchronous reluctance machine and an equivalent sized switched reluctance machine. The maximum torque per ampere trajectory is constant at a current angle of 45 degrees.

This also reflected in the high overload capability of the machine (Fig. 9), where at 300% rated current the torque maintains an almost linear relationship with current.

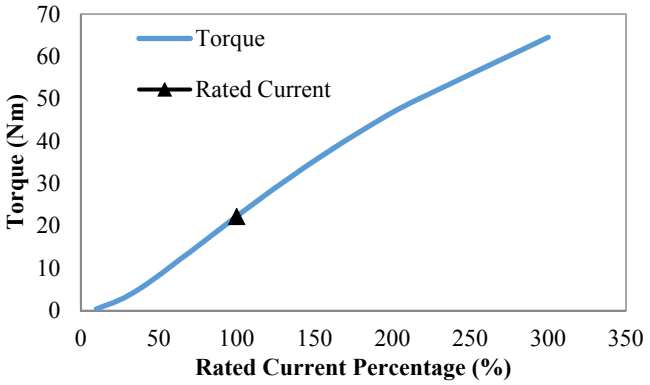

Fig.9. Torque vs. percentage line current, showing large overload capability.

Figure 10 shows the torque speed curves of the machine corresponding to current angles 45, 55, 65 and 75 degrees. The machine knee point is approximately 1500rpm and the top speed of the machine is around 8000rpm, giving a speed range of over 5 times the rated speed. This top speed is well within the maximum rotor speed of 10,000rpm. A current limit in Figure 8 is imposed of 21A, corresponding to 350W loss at the rated torque and speed.

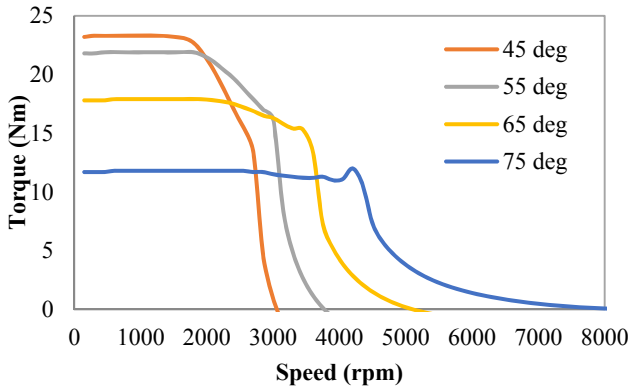

Fig.10. Torque vs. speed curves showing wide speed range.

The torque and line voltage waveforms are presented in Figure 11. It shows a good level of mean torque but a significant torque ripple (40%), even with an optimized rotor.

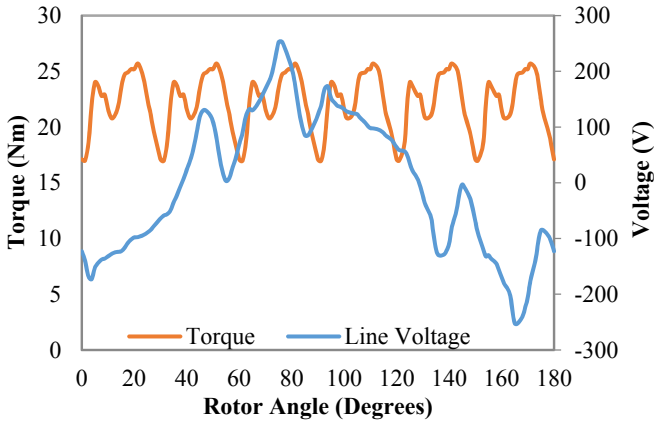

Fig.11. Torque and line voltage waveforms at rated operating point.

The line voltage waveform contains significant harmonic content – both of these parasitic effects are derived from the MMF space harmonics. The machine efficiency is 92% at rated operating point, the power factor is 0.47, which is low but agrees with the analytical work in Section III. This low power factor is caused by the excessive harmonic content in the airgap reducing the saliency ratio by increasing the leakage inductance. Also in Section III the average tangential stress was assumed to be 13kPa, where after finite element analysis a value of 12.4kPa is calculated, with is in line with the lower operating current. The fill factor aids the high efficiency, with a calculated winding loss of 299W and an iron loss of approximately 40W at the rated operating point. The machine is comparable (or even higher with certain designs) in torque density and torque per unit loss to some switched reluctance machines [10] however is driven from a conventional three phase voltage source inverter. The power factor of the developed cSynRM will be higher than the corresponding SRM.

VI. Prototype Machine

The designed machine has been prototyped and testing will further validate the performance calculated analytically and through finite element modelling. The stator component (showing short end windings) of the prototyped cSynRM is found in Fig. 12.

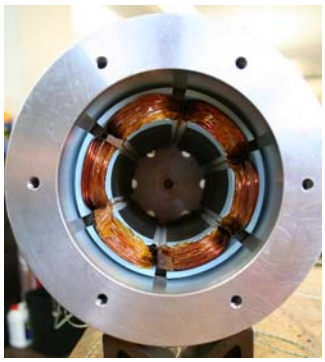

Fig.12. Stator component showing short end turns of the single tooth coils.

In Figure 12, the blue caps are CNC milled from Tufnell to the shape of the end winding, allowing a neat and tight coil to be wound without risk of shorts to the stator lamination stack. These are then wrapped with Kapton insulation tape for protection of the outer extremities of the end windings. A very short axial length (along shaft centre axis) of the end windings was achieved, only 19mm. A fill factor of approximately 60% was achieved, however recent work has shown that much high fills are possible [13] if the coils are precompressed. The rotor component was electro-discharge machined, a stator lamination is shown in Figure. 13.

Fig.13. Rotor lamination.

VII. Scaling and Future Development

This machine is highly scalable. The design can be scaled for larger outputs but also can be driven harder due to its high overload capability. However, adequate cooling would be required in demanding applications such as automotive, a water jacket and cooling system would accompany the motor. The major drawback is the machine power factor and its corresponding poor inverter utilization. This would limit its application in automotive where a fixed (usually low) battery voltage exists. Its robust and simple construction are advantageous in mass production and for application where durability and reliability are key design criteria. Future development can include addition of PM material into the design in order to improve the power factor of the machine and a scaled design for automotive traction applications. Minimisation of the effects of the space harmonics is also an area for further research.

VIII. Testing

Static and dynamic testing will confirm the finite element modelling. The aim of this paper was to present the concept of the machine and its design and performance based on analytical and numerical calculations, as well as present a prototype machine to provide and understanding that such a machine can be built and the fill factor achieved. Full experimental results will be presented in due course when they are available.

IX. Thermal Considerations

The insulation system is specified at Class F using grade II wire. The slot liner thickness is 0.3mm. In comparison to a conventionally wound synchronous reluctance machine with a large slot number (>36) the slot width of the cSynRM will be large, degrading the thermal path out of the winding – however the slot fill is significantly improved. The increase in achieved fill factor whilst lowering Joule loss will therefore act to reduce the hot spot temperature, despite this large slot width.

X. Conclusion

The paper has presented a 6 slot 4 pole synchronous reluctance motor with fractional-slot concentrated windings, known as the cSynRM. The machine is robust, relatively low cost and is easier to manufacture when compared to a conventional SynRM. High torque density and high efficiency with high overload capability are reported along with a wide speed range. The machine overcomes the previously reported low torque quality by better electromagnetic design of the rotor. However, the machine exhibits a poor power factor, which is the main disadvantage. Such a machine can be scaled to meet automotive power levels if adequate cooling is provided, such as a water jacket. Future development of this topology includes finding the best arrangement of ferrite based permanent magnets in the rotor to avoid demagnetization but aid power factor and torque production. Another avenue is to explore completely novel topologies of synchronous reluctance or permanent magnet assisted synchronous reluctance motors with short end windings.

Acknowledgment

The authors would like to thank Cummins Generator Technologies, Stamford, UK, for their financial assistance during the research project in which this paper is linked.

References

[1] Moghaddam, R.; Gyllensten, F., "Novel High Performance SynRM Design Method, an Easy Approach for a Complicated Rotor Topology," *Industrial Electronics, IEEE Transactions on* , vol.PP, no.99, pp.1,1, 0

[2] Moghaddam, R.R.; Magnussen, F.; Sadarangani, C., "Theoretical and Experimental Reevaluation of Synchronous Reluctance Machine," *Industrial Electronics, IEEE Transactions on* , vol.57, no.1, pp.6,13, Jan. 2010

[3] Bianchi, N.; Bolognani, S.; Bon, D.; Dai Pre, M., "Torque Harmonic Compensation in a Synchronous Reluctance Motor," *Energy Conversion, IEEE Transactions on* , vol.23, no.2, pp.466,473, June 2008

[4] Staton, D.A.; Miller, T. J E; Wood, S.E., "Maximising the saliency ratio of the synchronous reluctance motor," *Electric Power Applications, IEE Proceedings B* , vol.140, no.4, pp.249,259, Jul 1993

[5] Spargo, C.M.; Mecrow, B.C.; Widmer, J.D., "Application of fractional slot concentrated windings to synchronous reluctance machines," *Electric Machines & Drives Conference (IEMDC), 2013 IEEE International* , vol., no., pp.618,625, 12-15 May 2013

[6] Miller. T.J.E, 'Switched Reluctance Motors and Their Control', Magna Physics Press, 1991

[7] Spargo, C.M.; Mecrow, B.C.; Widmer, J.D., "Higher pole number synchronous reluctance machines with fractional slot concentrated windings," *Power Electronics, Machines and Drives (PEMD 2014), 7th IET International Conference on* , vol., no., pp.1,6, 8-10 April 2014

[8] EL-Refaie, A.M., "Fractional-Slot Concentrated-Windings Synchronous Permanent Magnet Machines: Opportunities and Challenges," *Industrial Electronics, IEEE Transactions on* , vol.57, no.1, pp.107,121, Jan. 2010

[9] C. M. Spargo, B. C. Mecrow and J. D. Widmer, 'A Semi-Numerical Finite Element Post-Processing Torque Ripple Analysis Technique for Synchronous Electric Machines Utilizing The Airgap Maxwell Stress Tensor', *Magnetics, IEEE Transactions on* , 2014

[10] Widmer, J.D.; Mecrow, B.C., "Optimized Segmental Rotor Switched Reluctance Machines With a Greater Number of Rotor Segments Than Stator Slots," *Industry Applications, IEEE Transactions on* , vol.49, no.4, pp.1491,1498, July-Aug. 2013

[11] Spargo, C.M.; Mecrow, B.C.; Widmer, J.D., "A Seminumerical Finite-Element Postprocessing Torque Ripple Analysis Technique for Synchronous Electric Machines Utilizing the Air-Gap Maxwell Stress Tensor," Magnetics, IEEE Transactions on , vol.50, no.5, pp.1,9, May 2014

[12] Magnussen, F.; Sadarangani, C.; , "Winding factors and Joule losses of permanent magnet machines with concentrated windings," Electric Machines and Drives Conference, 2003. IEMDC'03. IEEE International , vol.1, no., pp. 333- 339 vol.1, 1-4 June 2003

[13] Widmer, J.D.; Spargo, C.M.; Atkinson, G.J.; Mecrow, B.C., "Solar Plane Propulsion Motors With Precompressed Aluminum Stator Windings," *Energy Conversion, IEEE Transactions on* , vol.PP, no.99, pp.1,8
doi: 10.1109/TEC.2014.2313642